Journal of Power Sources 189 (2009) 585–589

Contents lists available at ScienceDirect

Journal of Power Sources

journal homepage: www.elsevier.com/locate/jpowsour

Short Communication

Mesoporous anatase TiO_2 composite electrodes: Electrochemical characterization and high rate performances

M. Mancini[a,b], P. Kubiak[a,*], J. Geserick[c], R. Marassi[b], N. Hüsing[c], M. Wohlfahrt-Mehrens[a]

[a] ZSW-Center for Solar Energy and Hydrogen Research, Helmholtzstraße 8, D-89081 Ulm, Germany
[b] Camerino University, Department of Chemical Sciences, Via S. Agostino 1, Camerino 62032, Italy
[c] Ulm University, Institute of Inorganic Chemistry I, Albert Einstein Allee 11, D-89081 Ulm, Germany

ARTICLE INFO

Article history:
Received 30 July 2008
Received in revised form
26 September 2008
Accepted 1 October 2008
Available online 22 October 2008

Keywords:
Mesoporous materials
Anatase TiO_2
Electrochemical lithium insertion

ABSTRACT

A metal film of Cu or Sn was vacuum-deposited on the surface of mesoporous anatase TiO_2 electrodes, and the Li insertion/extraction behaviour was investigated by cyclic voltammetry and galvanostatic cycling. The morphological and structural characterization of metal-coated electrodes showed that the metallic layers do not alter the structure of anatase. The electrode surface modification made by thin-film deposition improves the kinetics of Li insertion/extraction and remarkably enhances the electrochemical performances in terms of capacity and stability, especially at high charge/discharge rates.

1. Introduction

Many efforts have been directed towards improving Li-ion batteries especially in terms of energy and power content, lifetime, cost and safety. Many problems of the current configuration are related to the use of graphite-based anode, that present poor performances under some particular operating conditions, i.e. low temperatures and high charge/discharge rates, and high irreversible capacity in the first cycle due to the solid electrolyte interface (SEI) formation. Therefore there is an increasing interest in the development of alternative anode materials with enhanced kinetic and high rate capability. Anodic materials based on titanium oxides (e.g. TiO_2 or $Li_4Ti_5O_{12}$) are promising candidates as alternative materials to carbonaceous anodes, due to their important advantages in terms of cheapness, safety and toxicity with respect to other potential anodic materials. TiO_2 presents very interesting properties in the anatase structural type, with fast Li insertion/extraction reactions and high insertion capacity. The electrochemical Li insertion/extraction process has been extensively studied [1–5]. The theoretical capacity is 335 mAh g^{-1} corresponding to the insertion of 1 Li per mol of TiO_2. Practically about 0.5 Li at 1.78 V vs. Li/Li^+ (i.e. 168 mAh g^{-1}) can be reversibly inserted. Satisfactory results have been obtained by using nanosized anatase, which can be beneficial to both power rate and cycle life [6–9]. Indeed, nanosized anatase electrodes provide shorter pathway for both electronic and Li^+ transport, higher electrode–electrolyte contact area, and better accommodation of the strain of Li insertion/extraction. Mesoporous materials have received particular attention since they are effective in increasing the electrode stability and the Li insertion capacity especially at high charge/discharge rates [10–13]. The electronic conductivity can be increased by doping the active material with foreign atoms or by adding conductive phases [14–19]. In this context, we prepared mesoporous anatase electrodes modified by coating with an evaporated thin metal layer of Cu or Sn. The surface modification by thin film deposition of a metal layer presents important advantages in terms of easiness and cheapness when compared with other proposed optimization methods [14–16]. Electrode surface modification by metal layer deposition has been proven to be very effective in improving the charge/discharge rate of graphite-based systems and in protecting the electrode against solvent co-intercalation into the graphene layers [20–23].

In this study, the cycling behaviour of metal-coated electrodes has been compared with that of the unmodified mesoporous anatase electrodes in different experimental conditions, e.g. different potential ranges and several charge/discharge rates. The new metal/mesoporous anatase electrodes show excellent electrochemical performances in terms of capacity, cyclability, stability and reversibility, especially at high charge/discharge rates.

* Corresponding author. Tel.: +49 731 9530 401; fax: +49 731 9530 666.
E-mail address: pierre.kubiak@zsw-bw.de (P. Kubiak).

0378-7753/$ – see front matter © 2008 Elsevier B.V. All rights reserved.
doi:10.1016/j.jpowsour.2008.10.050

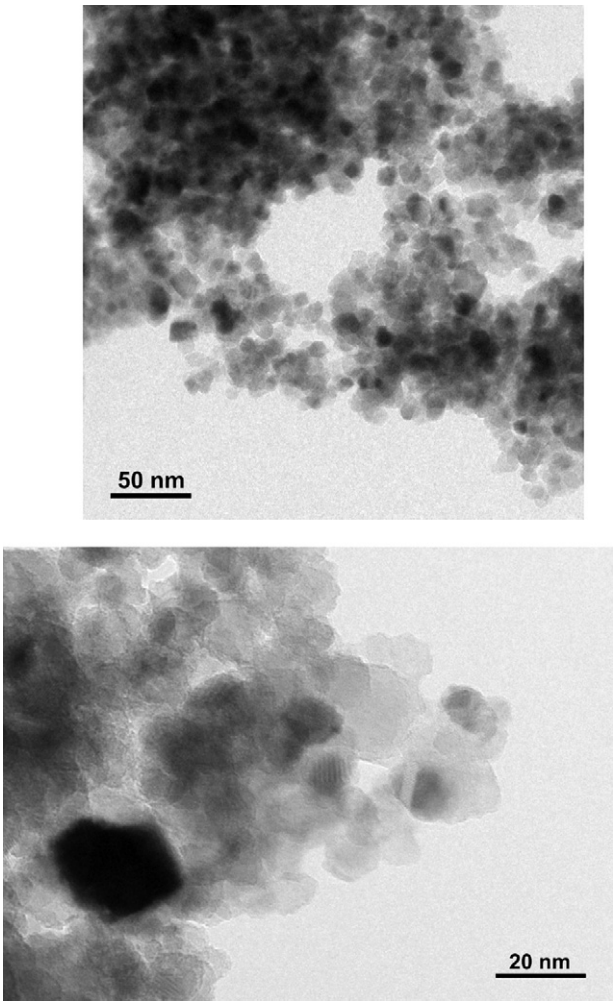

Fig. 1. TEM images of mesoporous TiO_2.

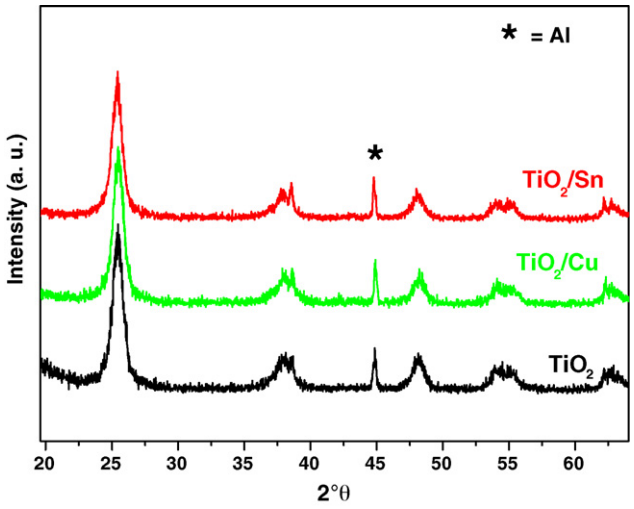

Fig. 2. X-rays diffractograms of the uncoated, Cu- and Sn-coated electrodes.

2. Experimental

2.1. Synthesis and characterization of mesoporous TiO_2

The synthesis of mesoporous anatase sample has been previously described in Ref. [13]. It has been prepared via a sol–gel method by precipitating bis(2-hydroxyethyl)titanate (EGMT) in acidic (pH 2) media in the presence of a non-ionic surfactant (Brij56, $M \sim 682\ g\ mol^{-1}$, Aldrich), followed by a thermal treatment at 400 °C under air.

Specific surface area of the mesoporous samples was calculated with a NOVA 4000e and Autosorp MP1 instrument (Quantachrome) analyzer based on the Brunauer–Emmet–Teller (BET) equation in the relative pressure (p/p_0) range of 0.05–0.3. The pore size distribution was determined according to Barrett, Joyner and Halenda (BJH) from the desorption branch of the isotherms.

2.2. Electrode preparation

The electrodes have been manufactured by preparing a slurry with the following composition: TiO_2:Super P:PVdF = 76:12:12 wt.%. The slurry was coated onto an Al foil as current collector using "doctor blade" technique (thickness 150 μm) and dried at 40 °C/1 h. The metal evaporation procedure was the same as described in [23]. The metal was allowed to evaporate onto the electrode surface applying a suitable current. The rate of the evaporation and the thickness (50 Å) of the deposited film were controlled by monitoring the deposited weight with a quartz crystal microbalance placed next to the sample. Circular electrodes were cut from the foil, pressed for better contact of the coated material and aluminum current collector and dried (130 °C) under vacuum overnight.

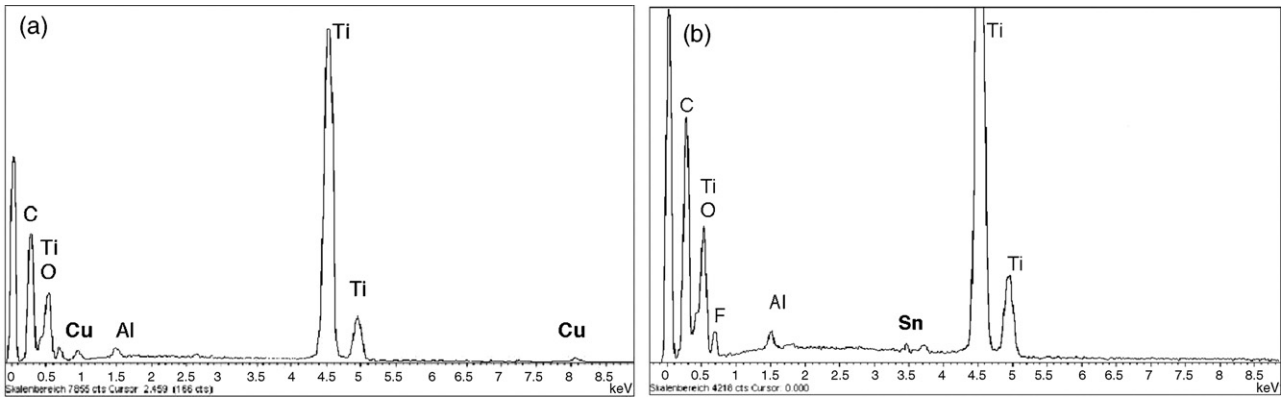

Fig. 3. EDX spectra of the Cu-coated (a) and Sn-coated (b) electrodes.

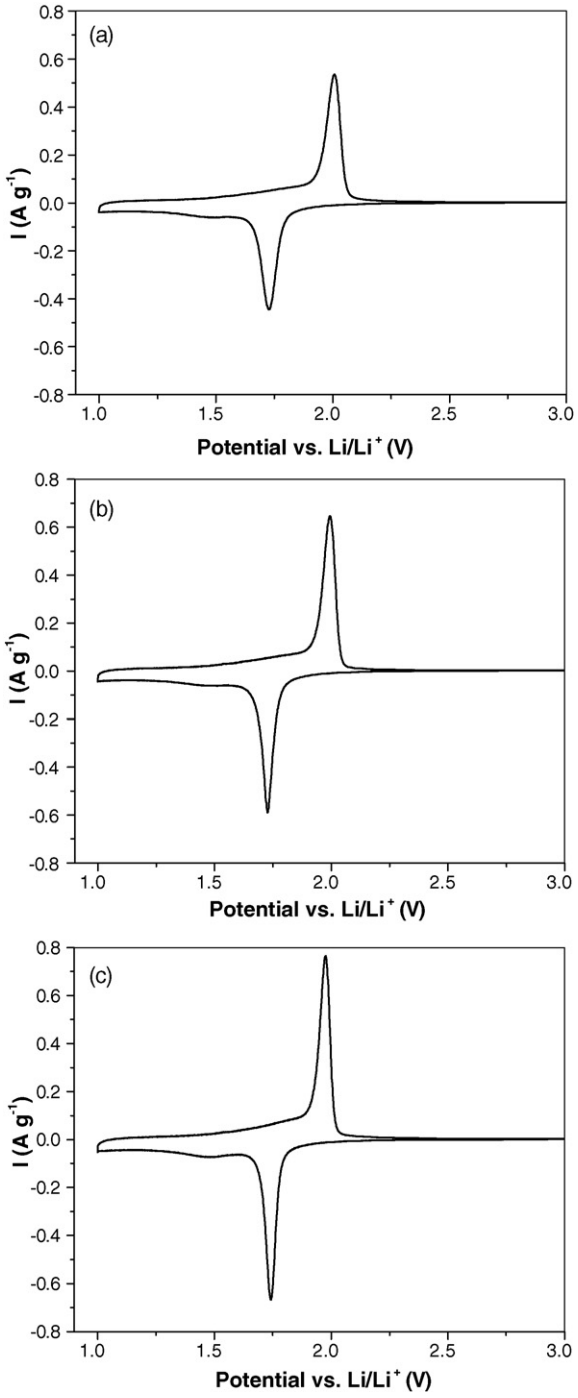

Fig. 4. Comparison between cyclic voltammograms (third cycle) of uncoated (a), Cu-coated (b), and Sn-coated (c) mesoporous TiO_2 at a scan rate $v = 0.1$ mV s^{-1}.

2.3. Structural and morphological characterization

Energy dispersive X-ray analysis (EDX) was performed on uncoated, Cu- and Sn-coated mesoporous TiO_2 samples on a LEO 1530 VP. Transmission electron microscopy (TEM) was performed on mesoporous TiO_2 on a Titan 80-300 at 80 kV. XRD measurements were performed using Cu-Kα radiation (λ = 0.154 nm) on a Siemens D5000.

2.4. Electrochemical characterization

The electrochemical measurements were performed using three-electrodes cells assembled in an argon-filled glove box (MBRAUN). Metallic lithium was used as reference and counter electrodes, glass microfiber (Whatman, GF/A) as separator and 1 M solution of LiPF6 in EC:DMC (1:1 by wt.%) (UBE Industry, Japan) as electrolyte. The maximum x in Li_xTiO_2 is assumed to be 0.5 (168 mAh g^{-1}) and thus, the charging rates in this measurements were based on the following relationship: $1C = 0.168$ A g^{-1}. All the measurements were carried out at room temperature using a VMP2/Z electrochemical workstation by PAR. All potentials are given vs. Li/Li^+.

3. Results

3.1. Material characterization

Mesoporous anatase TiO_2 sample with a BET specific surface area of 92 m^2 g^{-1} and a rather monomodal pore diameter close to 5 nm was used for anodes fabrication. The average crystallite size of the material, determined from diffraction peaks using the Scherrer's formula, is 9 nm which is in good agreement with the TEM image shown in Fig. 1. The good electrochemical behaviour of this material has been ascribed to its morphology, i.e. the high surface area and the mesoporosity [13].

3.2. Electrode characterization

The XRD characterization (Fig. 2) of the uncoated and of metal-coated electrodes showed a pure anatase phase with calculated cell parameters of $a = 3.785$ Å and $c = 9.514$ Å. The X-rays diffractograms of the different samples show the same peak position and shape, this indicating that the metal coating does not cause any modification in the anatase lattice parameters and in the crystallite size. As expected, no peaks due to either Cu or Sn are detected on the diffractograms due to the low quantity of metal deposited.

The presence of metal has been revealed by EDX analysis. The EDX spectrum (Fig. 3a) for the Cu-coated TiO_2 electrode shows the Cu-Kα and Lα peaks at 8.040 and 0.920 keV, respectively, corresponding to the deposited Cu. The EDX spectrum for the Sn-coated electrode (Fig. 3b) shows the peaks in the 3.400–4.100 keV range, corresponding to the deposited Sn. The metal content as determined by EDX analysis is less than 1 wt.% for both elements. The

Table 1
Summary of cycling data for uncoated, Cu- and Sn-coated anatase electrodes in different potential ranges (1.34 A g^{-1} charge/discharge rate).

	1–3 V			1.2–3 V			1.5–3 V		
	TiO_2	TiO_2–Cu	TiO_2–Sn	TiO_2	TiO_2–Cu	TiO_2–Sn	TiO_2	TiO_2–Cu	TiO_2–Sn
Q_{rev} (initial) (mAh g^{-1})	158.6	191.0	195.6	142.2	173.8	178.0	108.9	139.1	141.2
Q_{rev} (50 cycles) (mAh g^{-1})	132.4	156.8	156.8	128.6	156.6	157.0	112.8	135.7	137.5
Cap. ret. (%)	84	82	80	90	90	88	95[a]	98	97
ICL (mAh g^{-1})	30.5	31.9	27.3	19.7	14.0	15.2	10.9	8.5	6.2

[a] The maximum value of capacity (118.5 mAh g^{-1}) was reached after 13 cycles.

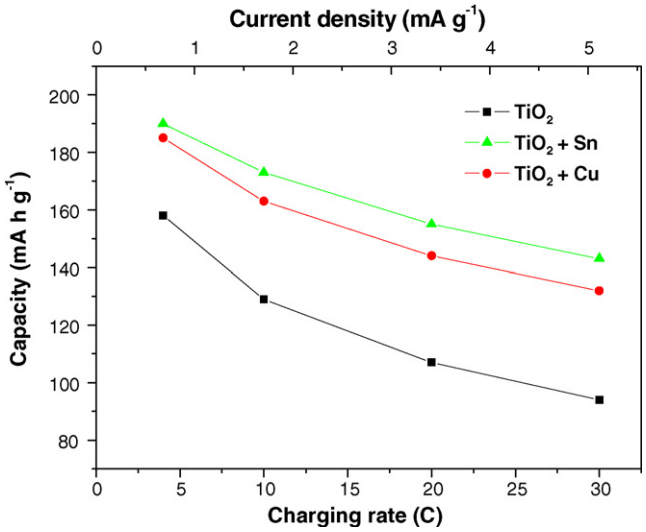

Fig. 5. Variation of reversible capacity of uncoated, Cu- and Sn-coated TiO_2 electrodes as function of charge/discharge rate. Potential range 1.2–3 V.

presence of the Al peak in both spectra is due to the Al foil used as current collector for the electrodes.

3.3. Cyclic voltammetry

Cyclic voltammetry has been carried out between 1 and 3 V on the uncoated, the Cu-and the Sn-coated electrodes at a scan rate of 0.1 mV s^{-1}. The comparison between the voltammograms is shown in Fig. 4. All three voltammograms present two peaks at about 1.75 V (cathodic) and 2.0 V (anodic) corresponding to the faradaic insertion and extraction of lithium into anatase TiO_2 [24].

Upon Li insertion, the anatase converts to a two-phase product, including the Li-poor $Li_{0.05}TiO_2$ (space group *I*41/*amd*) phase with tetragonal symmetry, and the Li-rich $Li_{0.5}TiO_2$ (space group *Imma*) phase with orthorhombic symmetry. The Li ions are randomly distributed over half of the available interstitial octahedral sites, leading to a Li storage capacity of 0.5 (168 mAh g^{-1}). Beside this faradaic process, taking place at about 1.78 V, other type of surface storage mechanisms, connected with pseudo-capacities, have been studied. These capacitive effects appear to be strictly connected with the dimensions, the porosity, and the surface areas of the material [6–8,25]. The voltammograms of metal-coated electrodes show higher and sharper current peaks and less peak separation than the uncoated one, suggesting better kinetics for metal-coated electrodes.

3.4. Galvanostatic experiments

It is known that the operating potential window has a large influence upon cyclability [13]. At potentials below 1.7 V, after all available interstitial sites in the bulk are occupied; the applied potential forces an additional topotactic Li insertion into surface layers. This further insertion mechanism leads to repulsive interactions between inserted Li with partial irreversible formation of short, covalent-type Li–O bonds and consequent strain in the lattice [5]. This Li storage process has been ascribed to the pseudo-capacitive contributions above described and is characterized by a progressive potential decrease below the plateau. Therefore it can be limited by controlling the operating potential window.

The electrochemical performances of the metal-coated mesoporous anatase electrodes have been evaluated by cycling in three different potential windows: 1–3, 1.2–3 and 1.5–3 V. The cycling stability has been evaluated under continuous insertion/extraction conditions at the 8*C* rate and the results for 50 cycles are summarized in Table 1. In all investigated potential ranges, the metal/anatase composite electrodes show higher capacity than the uncoated one. Nevertheless, the capacity and the stability depend on the applied cut off potential. If the potential is maintained at above 1.5 V, the further Li insertion after the faradaic process is limited, and a good stability of the material is obtained. In this potential

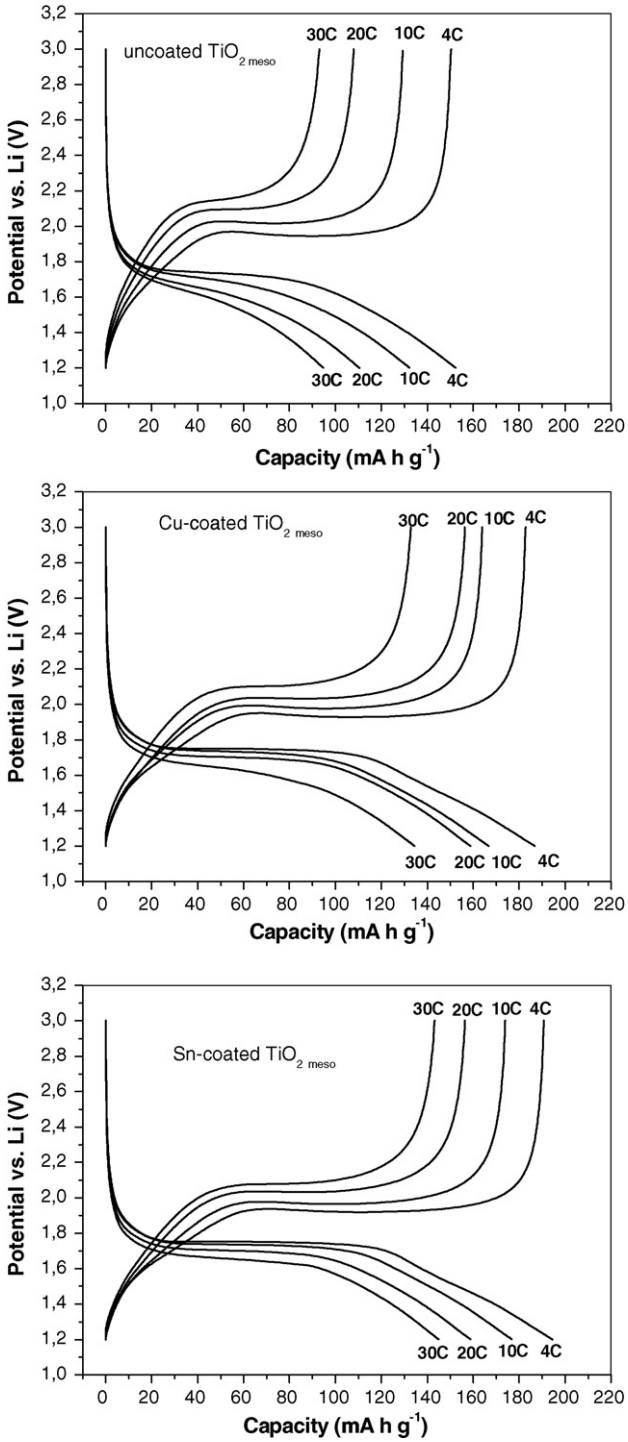

Fig. 6. Galvanostatic Li insertion/extraction curves at increasing current from 4*C* to 30*C* for the uncoated, the Cu- and the Sn-coated electrodes. Potential range 1.2–3 V.

range Li insertion/extraction is mostly controlled by the faradaic mechanism. At lower potentials a higher capacity is observed since both faradaic and capacitive contributions are involved. On the other hand, the capacity retention is lower due to a lower stability of the material. The effect of the capacitive contributions becomes more evident when the cut off is lowered from 1.2 V to 1 V. As expected, in the potential range 1–3 V all the electrodes show higher capacities but also lower stability. All the electrodes show similar values of capacity retention of about 80%, 90% and 98% in the potential windows 1–3, 1.2–3 and 1.5–3 V, respectively. The best compromise in terms of both cycling stability and high capacity is obtained by cycling between 1.2 and 3 V. The long-term stability upon cycling in this potential range has been evaluated. The capacity after 200 cycles is 123, 147 and 142 mAh g^{-1} for the uncoated, the Cu- and the Sn-coated anatase electrode, respectively, with capacity retention of about 80% for all electrodes. The applied cut off potential also influences the values of the irreversible capacity loss (ICL) during the first cycle, which decreases by decreasing the potential window. Nevertheless, the metal-coated electrodes show in general a lower ICL that the uncoated ones. The enhanced electrochemical behaviour of metal-coated electrodes is more evident when higher rates are used. The high rate performances of the electrodes have been studied by cycling at increasing current rates from 8*C* to 30*C* (Fig. 5). At the faster charge/discharge rate (30*C*, 5 A g^{-1}) the delivered capacities are 94, 132 and 143 mAh g^{-1} for the uncoated, the Cu- and the Sn-coated anatase electrodes, respectively.

Fig. 6 shows a comparison between galvanostatic Li insertion/extraction curves at increasing current from 4*C* to 30*C*. As expected, the increased polarization due to the increased charging rate leads to a shorter plateau associated with the biphasic region. By comparing the galvanostatic curves of the different electrodes we can observe two main effects related to the presence of the metal layer. The reversible capacities associated with faradaic process at the metal-coated electrodes are much higher than that of the pristine ones whichever the charging rate. The faradaic process is a solid-state mechanism, and thus it is highly dependent on the diffusion time. At 30*C* rate, the plateau of the uncoated electrode is very short and sloped, indicating losses in capacity, while those of the metal-coated electrodes are very well defined.

Moreover, the metal coating provides a lower polarization of the electrodes, this indicating faster kinetics of the electrochemical processes.

4. Discussion

The metal-coated electrodes showed better electrochemical performances than the pristine one. Any modification on the Li insertion/extraction mechanism due to the metallic layer was revealed neither by cyclic voltammetry nor by galvanostatic experiments. In every applied potential range the metal-coated electrodes show a capacity gain of about 30 mAh g^{-1} whichever the potential cut off, this suggesting that the metal coating effect is mostly related to the faradaic mechanism.

At present, the effect of the metal is not completely understood. Comparable results have been obtained in the case of metal-coated graphite-based electrodes [23] where the improved kinetics has been attributed mainly on a catalytic effect of the metal in accelerating the desolvation rate of lithium ions. However, anatase TiO_2 and graphite represent completely different systems based on two distinct Li storage mechanisms. For instance, in the case of Sn-coated graphite electrodes the intercalation is believed to occur through intermediate formation of Li–Sn alloy. This type of mechanism cannot take place in the present case since the potential range of Li–Sn alloys formation is never reached.

The presence of the metal is also associated with a lower capacity loss during the first cycle, which is generally attributed to irreversible surface reactions depending on the ionic and electronic conductivity of involved phases [8,15]. Therefore, the metal layer could influence surface reactions by improving the conductivity at electrolyte/active material interface. Other effects due to the metal, such as a decrease of the overall resistance cannot be excluded. These are at the moment under investigation and will be subject of a later communication.

5. Conclusion

The metal-coated electrodes show excellent electrochemical performances, especially in terms of fast insertion/extraction capacity.

The improved electrochemical behaviour is due to the combined effects of mesopores and of the electronically conductive metal layer.

The present study suggests that thin metal coating could be a very promising method in the development of high rate electrode materials for lithium-ion batteries.

Acknowledgements

Financial support from BMBF in the framework of the LISA project (03SF0327A) is gratefully acknowledged. The authors thank Prof. U. Kaiser and Dr. U. Hörmann, Ulm University, Institute for Electron Microscopy, for TEM experiments and fruitful discussions.

References

[1] A. Stashans, S. Lunell, R. Bergström, Phys. Rev. B 53 (1996) 159.
[2] L. Kavan, M. Grätzel, J. Rathouskỳ, A. Zukal, J. Electrochem. Soc. 143 (1996) 394.
[3] H. Lindstrom, S. Södergren, A. Solbrand, H. Rensmo, J. Hjelm, A. Hagfeldt, S.-E. Lindquist, J. Phys. Chem. B 101 (1997) 7717.
[4] M. Wagemaker, A. Kentgens, F. Mulder, Nature 418 (2002) 397.
[5] R. Baddour-Hadjean, S. Bach, M. Smirnov, J.-P. Pereira-Ramos, J. Raman Spectrosc. 35 (2004) 577.
[6] C. Jiang, M. Wei, Z. Qi, T. Kudo, I. Honma, H. Zhou, J. Power Sources 166 (2007) 239.
[7] M. Wagemaker, W.J.H. Borghols, F.M. Mulder, J. Am. Chem. Soc. 129 (2007) 4323.
[8] G. Sudant, E. Baudrin, D. Larcher, J.-M. Tarascon, J. Mater. Chem. 15 (2005) 1263.
[9] L. Kavan, J. Rathousky, M. Grätzel, V. Shklover, A. Zukal, J. Phys. Chem. B 104 (2000) 12012.
[10] L. Kavan, J. Rathousky, M. Grätzel, V. Shklover, A. Zukal, Micropor. Mesopor. Mater. 44–45 (2001) 653.
[11] Y.G. Guo, Y.S. Hu, J. Maier, Chem. Commun. 26 (2006) 2783.
[12] D. Fatthakova, M. Wark, T. Brezesinski, B. Smarsly, J. Rathousky, Adv. Funct. Mater. 19 (2007) 2087.
[13] P. Kubiak, J. Geserick, N. Hüsing, M. Wohlfahrt-Mehrens, J. Power Sources 175 (2008) 510.
[14] B.L. He, B. Dong, H.L. Li, Electrochem. Commun. 9 (2007) 425.
[15] Y.G. Guo, Y.S. Hu, W. Sigle, J. Maier, Adv. Mater. 19 (2007) 2087.
[16] I. Moriguchi, R. Hidaka, H. Yamada, T. Kudo, H. Murakami, N. Nakashima, Adv. Mater. 18 (2006) 69.
[17] H. Liu, L.J. Fu, H.P. Zhang, J. Gao, C. Li, Y.P. Wu, H.Q. Wu, Electrochem. Solid-State Lett. 9 (2006) A529.
[18] F. Nobili, S. Dsoke, T. Mecozzi, R. Marassi, Electrochim. Acta 51 (2005) 536.
[19] S.H. Huang, Z.Y. Wen, X.J. Zhu, X.L. Yang, J. Electrochem. Soc. 152 (2005) A1301.
[20] T. Takamura, K. Sumiya, J. Suzuki, C. Yamada, K. Sekine, J. Power Sources 81–82 (1999) 368.
[21] J. Suzuki, M. Yoshida, Y. Nishijima, K. Sekine, T. Takamura, Electrochim. Acta 47 (2002) 3881.
[22] L.J. Fu, H. Liu, C. Li, Y.P. Wu, E. Rahm, R. Holze, H.Q. Wu, Solid State Sci. 8 (2006) 113.
[23] F. Nobili, S. Dsoke, M. Mancini, R. Tossici, R. Marassi, J. Power Sources 180 (2008) 845.
[24] R. Van de Krol, A. Goossens, E. Meulenkamp, J. Electrochem. Soc. 146 (1999) 3150.
[25] J. Wang, J. Polleux, J. Lim, B. Dunn, J. Phys. Chem. C 111 (2007) 14925.